provides good scope for producing materials and coatings by vacuum condensation from plasma flows at high and adjustable particle energies [4-6, 11].

LITERATURE CITED

1. L. A. Artsimovich et al. (editors), Plasma Accelerators [in Russian], Mashinostroenie, Moscow (1973).
2. A. I. Morozov (editor), Physics and Applications of Plasma Accelerators [in Russian], Nauka i Tekhnika, Minsk (1974).
3. A. M. Dorodnov, "Some applications of plasma accelerators in technology," in: Physics and Applications of Plasma Accelerators [in Russian], Nauka i Tekhnika, Minsk (1974).
4. I. G. Blinov, A. M. Dorodnov, V. E. Minaichev, et al., High-Current Vacuum Plasma Devices and Applications in Microelectronic Equipment. Part 2. High-Energy Plasma Technology. Surveys on Electronics [in Russian], Izd. TsNII Elektronika, No. 8, Moscow (1974).
5. A. M. Dorodnov, Industrial Plasma Sources (Textbook) [in Russian], N. E. Bauman Moscow Higher Technical School (1976).
6. I. G. Blinov, A. M. Dorodnov, V. E. Minaichev, et al., High-Current Vacuum Plasma Devices and Applications in Microelectronic Equipment. Part 1. Physical Principles. Surveys on Electronics [in Russian], No. 7, Izd. TsNII Elektronika, Moscow (1974).
7. U.S. Patent, class 204-192, No. 3,625,848 (1971).
8. V. E. Minaichev and S. I. Miroshkin, Stationary High-Current Plasma Evaporators for Metals and Alloys. Surveys on Electronics [in Russian], No. 5, Izd. TsNII Elektronika, Moscow (1975).
9. L. P. Sablev, Yu. I. Dolotov, et al., "An electric arc evaporator for metals with magnetic stabilization of the cathode spot," Prib. Tekh. Eksp., No. 4 (1976).
10. British Patent, class C7F, No. 1,322,670 (1973).
11. A. G. Tumanov, V. N. Barabanov, A. M. Dorodnov, et al., "Effects of ion energy and condensation rate on the structures of vacuum coatings," in: Abstracts for the Third All-Union Conference on Plasma Accelerators [in Russian], Minsk (1976).

AN ELECTROSTATIC WALL PROBE IN A FLOW OF COOL PLASMA

É. K. Chekalin and L. V. Chernykh

UDC 538.4

There are various difficulties in using an electrostatic wall probe with a flow of relatively dense plasma on account of convection and the formation of temperature and hydrodynamic boundary layers, as well as ambipolar diffusion, discrepancies between the electron temperature and the gas temperature, and nonequilibrium ionization and electron–ion recombination.

A major task in theoretical examination of the properties of wall probes is to construct voltage–current characteristics and determine the relation between the saturation ion current and the electrophysical parameters of the unperturbed plasma. The available data are conflicting. In [1-3], the saturation ion current was dependent on the profiles of the electron and gas temperatures near the probe. On the other hand, it follows from [4-6] that there is no appreciable effect on the saturation current from the distributions of these temperatures at the surface.

To resolve these conflicts and to provide a sound basis for the use of wall probes it is necessary to determine the theoretical distributions for the charged-particle concentrations, electric fields, and electronic and ionic components of the probe current together with the voltage–current characteristics, although it is extremely complicated to consider all the above factors [7]. For this reason, various simplifications and assumptions were made. For example, convection was neglected in [7-10], while the nonequilibrium ionization and recombination processes in the boundary layer were neglected in [11]. However, these simplifications are not always reasonably justified, and the limits of application are frequently not stated.

Moscow. Translated from Zhurnal Prikladnoi Mekhaniki i Tekhnicheskoi Fiziki, No. 1, pp. 41-47, January-February, 1981. Original article submitted July 18, 1979.

0021-8944/81/2201-0032$07.50

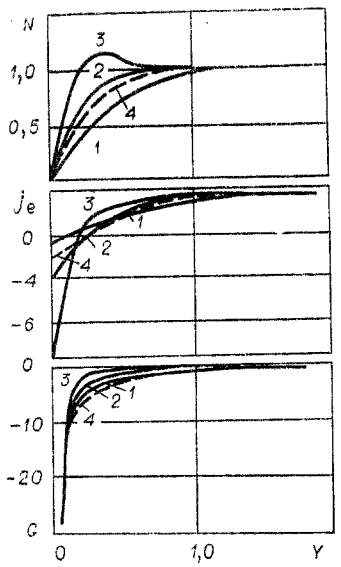

Fig. 1

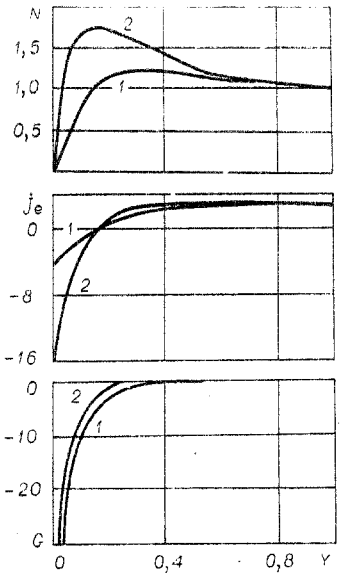

Fig. 2

Here we derive the charged-particle concentration profiles, the electric field, and the electron component of the probe current for various profiles in the electron and gas temperatures, and also for various relations between the characteristic times of diffusion and electron–ion recombination and various values of the total probe current in a quasineutral ambipolar part of the boundary layer.

The data provide the saturation ion current and the voltage–current characteristics, as well as the boundary conditions for the double electric layer at the electrode surface.

The following is a system of differential equations for the flows of charged particles from the source to the quasineutral region of the boundary layer in a flow of low-temperature plasma for $T_e \neq T_i$:

$$\rho\frac{\partial C_i}{\partial t}+\rho u\frac{\partial C_i}{\partial x}+\rho v\frac{\partial C_i}{\partial y}=\frac{\partial}{\partial y}\left(\rho D_i\frac{\partial C_i}{\partial y}-\rho\mu_i EC_i\right)+\dot{\omega}_i M_i; \tag{1}$$

$$\rho\frac{\partial C_e}{\partial t}+\rho u\frac{\partial C_e}{\partial x}+\rho v\frac{\partial C_e}{\partial y}=\frac{\partial}{\partial y}\left\{\rho D_e\frac{T_i}{T_e}\frac{\partial}{\partial y}\left(\frac{C_eT_e}{T_i}\right)+\rho\mu_e EC_e\right\}+\dot{\omega}_e M_e, \tag{2}$$

where ρ is the plasma density; u and v, gas speeds in the x and y directions, respectively; y, normal to the surface of the electrode; t, time; $C_{i,e}$, mass proportions of ions and electrons, respectively; $D_{i,e}$, diffusion coefficients; $\mu_{i,e}$, mobility coefficients; E, strength of the electric field in the direction of the y axis; $T_{i,e}$, temperature; $\dot{\omega}_{i,e}$, rate of ionization and recombination; and $M_{i,e}$, masses of the charged particles.

Here it is assumed that $C_i = C_e$, $T_i = T_a$ and the profiles for the electron and gas temperatures have been derived by solving the energy equations for the electrons and gas in the boundary layer. In the case $T_e = T_i$, (1) and (2) can also be used. We consider two models: frozen electron temperature $T_e = T_{a\infty}$ and equilibrium electron temperature $T_e = T_a$ everywhere in the quasineutral region of the boundary layer. It is further supposed that the thickness of the double electrical layer is negligible by comparison with that of the concentration boundary layer, and that the charged-particle density at the outer boundary of the electrical layer is negligible by comparison with that in the unperturbed plasma, that the degree of ionization is small, and that the problem can be treated in the one-dimensional approximation, while energy dissipation can be neglected, there is no electron-emission current, the transport coefficients are dependent on the electron and ion temperatures, and the electron–ion recombination is of three-particle type, $(A + e^- \rightleftarrows A^+ + 2e^-)$.

In solving (1) and (2) it is assumed as in [7-10] that the convective terms on the left can be neglected. However, here we define the limits to the application of this. The assumption is quite justified for a sufficiently large value of the $\dot{\omega}_{i,e}M_{i,e}$ term, which corresponds to the Damkeller number $B = \tau_d/\tau_r \geqslant 10$, where $\tau_{d,r}$ are the characteristic diffusion and recombination times respectively, with this term exceeding the values of the convective terms by at least an order of magnitude, which was demonstrated by estimating the terms in (1) and (2) as reduced to dimensionless form in the models $T_e = T_{a\infty}$, $T_e = T_a$.

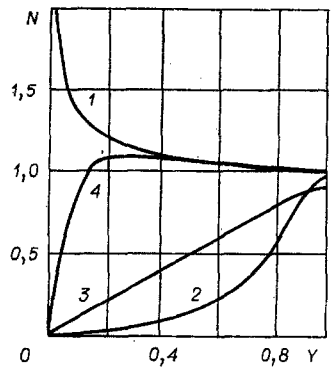

Fig. 3

We neglect the convective terms in (1) and (2) and use the constancy of the total probe current in the boundary layer with the above assumptions to get after integration that

$$F_e = -\left[D_e n_a T_i/T_e \cdot \frac{d\,(n_e/n_a \cdot T_e/T_i)}{dy} + \mu_e n_e E\right]; \tag{3}$$

$$F_i = -\left[D_i n_a \frac{d\,(n_i/n_a)}{dy} - \mu_i n_i E\right]; \tag{4}$$

$$i = e(F_i - F_e); \tag{5}$$

$$\dot{\omega}_{i,e} = \frac{dF_{i,e}}{dy} = k_1 n_a n_e - k_2 n_i n_e^2, \tag{6}$$

where $F_{i,e}$ are the charged-particle fluxes; $n_{i,e,a}$, concentrations of the ions, electrons, and neutral particles, respectively; i, probe current; e, electronic charge; and $k_{1,2}$, ionization and recombination constants, respectively.

We consider two cases: the gas temperature profile in a laminar boundary layer in a shock tube [12] and a linear distribution simulating the laminar sublayer in a turbulent boundary layer.

We reduce (3)-(6) to dimensionless form following [9].

In the case $T_e = T_{a\infty}$, system (3)-(6) becomes

$$\frac{dN}{dY} = -\frac{j_e\left(\gamma_\infty + \Theta^{1/2}\right) - j\Theta^{1/2}}{(1+\Theta)\,\Theta} - \frac{N}{(1+\Theta)}\frac{d\Theta}{dY}; \tag{7}$$

$$\frac{dj_e}{dY} = BN\left(\frac{1}{\Theta} - N^2\right); \tag{8}$$

$$G = \frac{j + j_e\left(1 - \gamma_\infty \Theta^{1/2}\right)}{N\Theta^{1/2}\,(1+\Theta)} + \frac{1}{(1+\Theta)}\frac{d\Theta}{dY}, \tag{9}$$

where $j = j_i - j_e$; $N = n_e/n_{e\infty}$; $Y = y/\delta$; $j_{i,e} = F_{i,e}\delta/n_{e\infty}D_{i\infty}$ (δ is the thickness of the temperature boundary layer), $\gamma_\infty = \mu_{i\infty}/\mu_{e\infty}$; $\Theta = T_a/T_{a\infty}$; $\mu_{i,e} = eD_{i,e}/kT_{i,e\infty}$; $B = \delta^2 k_{2\infty} n_{e\infty}^2/D_{i\infty}$; $G = e\delta E/kT_{a\infty}$.

In the case $T_e = T_a$, (3)-(6) becomes

$$\frac{dN}{dY} = \frac{-j_e(\gamma_\infty + 1) - j}{2\Theta^{3/2}} - \frac{N}{\Theta}\frac{d\Theta}{dY}; \tag{10}$$

$$\frac{dj_e}{dY} = BN\frac{1}{\Theta^{9/2}}\left[\Theta^{1/2}\exp\left(-\frac{U_i}{kT_\infty}\frac{(1-\Theta)}{\Theta}\right) - N^2\right]; \tag{11}$$

$$G = \frac{j_e(1-\gamma_\infty) + j}{2N\Theta^{1/2}}, \tag{12}$$

where $j = j_i - j_e$ and U_i is the ionization potential.

Systems (7)-(9) and (10)-(12) are solved with the following boundary conditions: $N = 0$, $j_e = j_{ew}$ for $Y = 0$ and $N \to 1$, $j_e \to j$ for $Y \to \infty$. The problem has been solved for various currents, Damkeller numbers, and two different temperature distributions $\Theta(Y)$.

Systems (7)-(9) and (10)-(12) were solved numerically with a BÉSM-6 computer by the Runge—Kutta method with a step $\Delta Y = 0.04$.

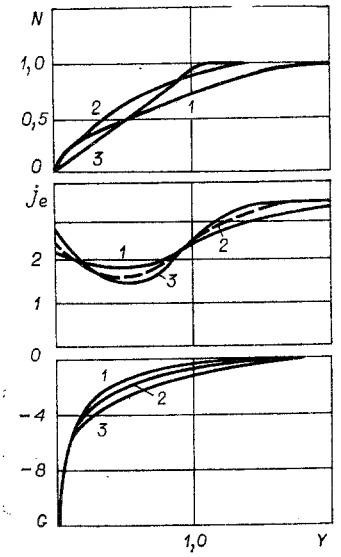

Fig. 4

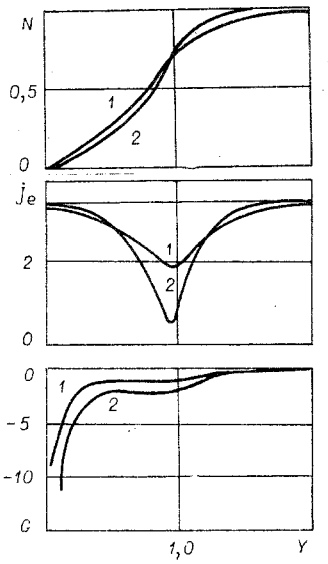

Fig. 5

In the program, the electron current j_{ew} at the wall was specified as an array of values, and a solution was found for each of them with given values of j and B and a given $\Theta(Y)$. From the solutions we selected the one that satisfied the boundary conditions $N \to 1$ and $j_e \to j$ for $Y \to \infty$ [13].

Figures 1 and 2 give numerical results for $T_e = T_{a\infty}$, $j = -3.5$ for the laminar gas-temperature profile (Fig. 1) and the linear one (Fig. 2) (1 — B = 10, 2 — B = 30, 3 — B = 100); Figs. 1 and 2 imply that B markedly influences $N(Y)$, $j_e(Y)$ when $T_e = T_{a\infty}$. A distinctive feature of $N(Y)$ is provided by the peaks for $N > 1$, which is due to ionization and charged-particle recombination in the boundary layer with an inhomogeneous gas density, as is evident from data given in Fig. 3, which indicates the limiting equilibrium profile $N(Y)$ for $B \to \infty$ (curve 1) as calculated from Saha's formula for $T_e = T_{a\infty}$:

$$N = \Theta(Y)^{-1/2}. \tag{13}$$

Figure 3 also shows $N(Y)$ for $T_e = T_{a\infty}$ for B = 100 (curve 4).

This shows that N increases towards the wall as $\Theta(Y)$ decreases; the concentration profile approximates to an equilibrium distribution ($\tau_r \to 0$) as B increases, while for $B \to 0$ the profile is close to a frozen one and is determined only by diffusion processes ($\tau_d \to 0$).

The profile for $N(Y)$ becomes flatter as B increases and the saturation ion current ($j_i^s = j + j_{ew}$) increases considerably for Y = 0.

Curves 4 of Fig. 1 show analytic solution to (7)-(9) of [9] for B = 30 for $T_e = T_a = T_{a\infty}$ (Θ = const), i.e., in the absence of a temperature boundary layer. The profiles for B = 30 for $T_e = T_{a\infty}$ and $T_e = T_a = T_{a\infty}$ show that an inhomogeneous thermal boundary layer has little effect on the distributions of $N(Y)$, $j_e(Y)$, and $G(Y)$, and the saturation ion current for $T_e = T_a = T_{a\infty}$ is lower than that for a laminar temperature layer, i.e., the saturation ion current falls as the wall temperature Θ_w increases.

The numerical calculations show that variations in probe current j in the range from −1 to −7 for $T_e = T_{a\infty}$ have virtually no influence on $N(Y)$, $j_e(Y)$, and $G(Y)$.

Figures 1 and 2 show that the distribution of $N(Y)$ are flatter for a linear distribution $\Theta(Y)$, while the saturation ion currents are considerably higher than for a laminar layer, which can also be explained via (13).

Figures 4 and 5 show theoretical $N(Y)$, $j_e(Y)$, and $G(Y)$ curves for a laminar gas-temperature profile (Fig. 4) and a linear one (Fig. 5) in the boundary layer for $T_e = T_a$ (the symbols and the magnitude of j are analogous to Figs. 1 and 2). Figures 4 and 5 imply that B has little effect on $N(Y)$, while the electron component of the current j_e has a minimum in the range of Y from 0 to 1. One cannot neglect the convective terms in (1) for $T_e = T_a$ near this minimum, but check calculations of (1) without the term containing the electric field E, which has virtually no effect on the ions, have shown that the saturation ion currents at the surface of the electrode in that case differ by 1-2% from the case where the convective terms are neglected.

TABLE 1

		$T_a(Y)$ lam		$T_a(Y)$ lin		$T_e = T_a = T_{a\infty}$
		$T_e = T_a$	$T_e = T_{a\infty}$	$T_e = T_a$	$T_e = T_{a\infty}$	
B	j	V	V	V	V	V
10	−3,5	−2,32	−2,75	−2,7	−1,92	−2,76
30	−1,0	−2,43	−2,45	—	—	−2,2
30	−3,5	−2,30	−1,51	−3,12	−1,32	−2,2
30	−7,0	−2,42	−1,72	—	—	−2,2
100	−3,5	−2,58	−0,84	—	—	−1,6

The N(Y) curves for the various B lie near the equilibrium distribution for $B \to \infty$ (curve 2 in Fig. 3), which corresponds to Saha's formula for $T_e = T_a$:

$$N = \frac{1}{\Theta(Y)^{1,2}} \exp\left\{-\frac{U_i}{kT_{e\infty}} \frac{[1-\Theta(Y)]}{\Theta(Y)}\right\}.$$

For comparison, Fig. 3 shows N(Y) for $T_e = T_a$ for B = 100 (curve 3).

Figures 4 and 5 also show that the saturation ion currents are only very slightly dependent on B. A difference from the case $T_e = T_{a\infty}$ is that the ion current falls as B increases, i.e., the magnitude of the current is small by comparison with the case $T_e = T_{a\infty}$. For a linear $\Theta(Y)$ with $T_e = T_a$ we get ion currents far smaller than those for a laminar boundary layer. The effects of B on G(Y) are slight. The value of j in the range from −1 to −7 had almost no effect on the profiles. For $T_e = T_a$ the thickness of the concentration boundary layer exceeded the thickness of the temperature layer, and the difference in thicknesses between these layers increased as B decreased.

The analytic solution for B = 30 in Fig. 1 goes with the data of Fig. 4 to show that a difference from the case $T_e = T_{a\infty}$ is that the saturation ion current increases with Θ_w, which confirms the results of [4].

One can judge the difference between the electron temperature and the gas temperature in the boundary layer from the dependence of the saturation ion current on B and Θ_w.

Numerical integration of G(Y) derived in the calculations gives the dimensionless potential difference:

$$V = -\int_h^1 G dY = -\frac{eU}{kT_{e\infty}}.$$

Table 1 gives results from numerical integration of G(Y) for various B and j and various electron and gas temperature profiles. Table 1 shows that V for $T_e = T_a$ in the laminar layer is almost independent of j and B. For $T_e = T_{a\infty}$ and $T_e = T_a = T_{a\infty}$ we find that $|V|$ decreases as B increases for constant j of −3.5. For a linear distribution of $\Theta(Y)$ with $T_e = T_{a\infty}$ we find that $|V|$ is lower than for a laminar layer, while $T_e = T_a$ gives $|V|$ higher than this.

Comparison of the voltage–current characteristics for a uniform temperature distribution ($T_e = T_a = T_{a\infty}$) and for the cases $T_e = T_{a\infty}$ and $T_e = T_a$ shows that the resistance of the ambipolar region in the boundary layer for $B > 10$ and $|j| > 1$ is higher than for $T_e = T_{a\infty}$ and lower than that for $T_e = T_a$.

These estimates of the quasineutrality of the ambipolar region can be used on the basis of the conditions of the experimental tests to demonstrate a high degree of quasineutrality in the plasma down to Y = 0.04, which satisfies

$$(N_i - N_e)/N_i \simeq 10^{-3} \ll 1.$$

There are deviations from quasineutrality only in the region of the space-charge layer for $Y \simeq 10^{-3}$, where no calculations were performed.

Some of the calculations have been compared with the experimental data derived from a shock tube with a supersonic flow of shock-heated argon plasma [14, 15].

The Mach number of the shock wave varied from 8 to 12, while the initial pressure varied from 1 to 50 mm Hg, and the gas pressure behind the shock wave varied from 0.3 to 5 atm, while

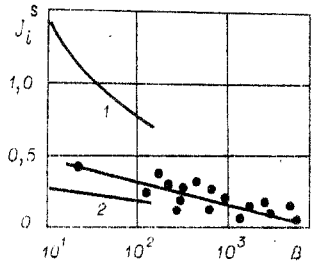

Fig. 6

the electron concentration varied from 10^{14} to 10^{16} cm^{-3}, the thickness of the laminar boundary layer from 0.15 to 0.5 cm, and the recombination coefficient $k_{2\infty}$ varied from 10^{-26} to $7 \cdot 10^{-26}$ $cm^6 \cdot sec^{-1}$.

The electron concentration in the unperturbed flow was determined on the basis of the ionization relaxation behind the shock wave. The wall probes were electrodes placed on opposite walls of an insulating measuring section. The observed voltage–current characteristics were used to determine the saturation ion currents. The value of B for the points was calculated from the conditions in the plasma flow behind the shock wave.

Figure 6 shows observed and calculated relationships between the dimensionless saturation ion current and the parameter B (1 — Θ_w = 0.13, 2 — Θ_w = 0.05); the conditions of the experiments corresponded to Θ_w = 0.05.

The fall in j_i^s as B increases indicates equality of the two temperatures ($T_e = T_a$); however, the weak dependence of j_i^s on B does not allow one to determine $n_{e\infty}$ accurately [15].

The discrepancy between the theoretical data (Θ_w = 0.05) and the observations is probably due to the assumptions, whose correctness is not always obvious. For example, the degree of ionization cannot be considered as small for some of the experiments, while the electron concentration at the wall is probably different from zero, and so on.

Therefore, these numerical calculations on the electrical properties of the boundary layers give a qualitative indication of the saturation ion currents to an electrostatic probe and the level of difference between the electron temperature and the gas temperature in the ambipolar region of the boundary layer when there is recombination in the plasma.

LITERATURE CITED

1. N. Stahl and C. H. Su, "Theory of continuum flush probes," Phys. Fluids, 14, No. 7 (1971).
2. R. E. Kiel, "Electrostatic probe theory for free molecular cylinders," AIAA J., 6, No. 4 (1968).
3. C. S. Su and S. H. Lam, "Continuum theory of spherical electrostatic probes," Phys. Fluids, 6, No. 10 (1963).
4. P. M. Chung, L. Talbot, and K. J. Touryan, "Electric probes in stationary and flowing plasmas. Part 2. Continuum probes," AIAA J., 12, No. 2 (1974).
5. B. Zauderer and E. Tate, "Electrical characteristics of a linear, nonequilibrium, MHD generator," Proc. IEEE, 56, No. 9 (1968).
6. D. L. Thomas, "Continuum theory of cooled spherical electrostatic probes," Phys. Fluids, 12, No. 2 (1969).
7. D. T. Shaw, "Behavior of relaxation plasmas near emitting surfaces," Energy Convers., 11, No. 3 (1971).
8. V. Yu. Baranov, D. D. Malyuta, and F. R. Ulinich, "Current transmission through boundary layers," Teplofiz. Vys. Temp., 11, No. 3 (1973).
9. G. A. Lyubimov and V. I. Mikhailov, "Analysis of the perturbation region near an electrode," Izv. Akad. Nauk SSSR, Mekh. Zhidk. Gaza, No. 3 (1968).
10. A. L. Genkin and A. D. Lebedev, "Diffusion of charged particles in a boundary layer on an electrode," Magn. Gidrodin., No. 2 (1969).
11. P. M. Chung and V. D. Blankenship, "Theory of electrostatic double probe comprised of two parallel plates," AIAA J., 4, No. 4 (1966).
12. R. E. Duff, "Laminar boundary layer. Development behind shock waves in argon," Phys. Fluids, 1, No. 6 (1958).

13. E. K. Chekalin and L. V. Chernykh, "Electrophysical properties of temperature boundary layers at electrodes in a flow of conducting gas," in: MHD and Electrophysical Characteristics of Conducting-Gas Flows [in Russian], Issue 8, Minenergo SSSR, Glavniiproekt, Moscow (1973).
14. E. K. Chekalin, L. V. Chernykh, M. A. Novgorodov, and N. V. Khandurov, "Determination of the electron concentration in a supersonic plasma flow by means of a wall electrostatic probe," in: Proceedings of the All-Union Symposium on Aerophysical Research Methods [in Russian], Izd. ITPM Sib. Otd. Akad. Nauk SSSR, Novosibirsk (1976).
15. E. K. Chekalin, M. A. Novgorodov, and N. V. Khandurov, "Effects of electron–ion recombination in the boundary layer on the readings of an electrostatic probe," Zh. Tekh. Fiz., 45, No. 7 (1975).

CALCULATION OF THE VOLT–AMPERE CHARACTERISTICS OF A NONINDEPENDENT VOLUMETRIC ELECTRICAL DISCHARGE

V. V. Aleksandrov and V. N. Diesperov

UDC 537.5

An analysis of a nonindependent volumetric electrical discharge in the phase plane makes it possible to describe the structure of this phenomenon in a very simple manner and construct the volt–ampere characteristics over a broad range of parameters.

1. A volumetric electrical discharge in a dense gas induced by hard ultraviolet rays, x rays, reactor radiation, or a beam of fast electrons is widely used in the design of operating chambers of high-powered electroionization gas lasers [1, 2] and high-current switching devices [3]. This discharge can be simulated by a plane capacitor which has fairly high voltage applied to its plates. The space between the electrons is filled with a gas which has a temperature of the same order as room temperature and is weakly ionized as a result of an external source, e.g., an electron beam. Given a number of assumptions, which are reasonably well satisfied for modern lasers [1, 2, 4], a nonindependent stationary volumetric electric discharge can be described by the following system of equations for the electrons and ions moving in a fixed gas consisting of neutral particles:

$$\frac{dj_e}{dx} = -\frac{dj_i}{dx} = j_e\alpha + q - \beta n_e n_i,$$
$$\frac{dE}{dx} = 4\pi |e| (n_e - n_i),\ j_e = \mu_e n_e E/p,\ j_i = \mu_i n_i E/p, \qquad (1.1)$$
$$j_e(0) = \gamma j_i(0),\ j_i(1) = 0,\ \int_0^L E dx = U.$$

Here the coordinate x is measured from the cathode (x = 0) to the anode (x = 1); j_e and j_i, densities of the electron and ion currents; n_e and n_i, electron and ion densities. The electron and ion currents vary as a result of the impact ionization of neutral particles by electrons, which is proportional to the density of the electron current multiplied by the impact generation function α, to the external ionization, whose intensity q will be assumed to be a known quantity, and to the binary recombination, equal to the product $n_e n_i$, with a proportionality constant β, known as the first Townsend coefficient. In the drift approximation under consideration, the currents j_e and j_i are proportional to the intensity E of the electric field, where μ_e and μ_i are the mobilities of the electrons and the ions [5] and p is the pressure of the neutral gas. The equation for the field E, in which e denotes the charge of the electron, closes this system. The ion bombardment of the cathode results in the emission of electrons from the cathode, which is characterized by the value γ, the second Townsend coefficient. The ion current at the anode is equal to zero. A potential difference U is maintained across the plates of the capacitor.

For the impact generation function α the two most widely used approximations are the following [5]:

Moscow. Translated from Zhurnal Prikladnoi Mekhaniki i Tekhnicheskoi Fiziki, No. 1, pp. 48-60, January-February, 1981. Original article submitted November 20, 1979.

 0021-8944/81/2201-0038$07.50